

# Segmented swept source optical coherence tomography angiography assessment of the perifoveal vasculature in patients with X-linked juvenile retinoschisis: a serial case report

Francesco Stringa<sup>1,2</sup>  
Emmanouli Tsamis<sup>1,3</sup>  
Alessandro Papayannis<sup>1</sup>  
Katarzyna Chwiejczak<sup>1</sup>  
Assad Jalil<sup>2</sup>  
Susmito Biswas<sup>1,2,4</sup>  
Hassan Ahmad<sup>1</sup>  
Paulo Eduardo Stanga<sup>1,2,4</sup>

<sup>1</sup>Manchester Vision Regeneration (MVR) at NIHR/Wellcome Trust Manchester Clinical Research Facility,

<sup>2</sup>Manchester Royal Eye Hospital, Central Manchester University Hospitals NHS Foundation Trust, Manchester Academic Health Science Centre, <sup>3</sup>Division of Pharmacy and Optometry, School of Health Sciences, <sup>4</sup>Division of Evolution and Genomic Sciences, School of Biological Sciences, Faculty of Biology, Medicine and Health, The University of Manchester, Manchester Academic Health Science Centre, Manchester, UK

**Purpose:** To describe perifoveal microvascular changes occurring in X-linked juvenile retinoschisis (XLRS) using swept source optical coherence tomography angiography (SS OCTA).

**Patients and methods:** This is a serial case report of three patients. Retrospective data of patients affected by XLRS were collected. Structural optical coherence tomography (OCT) and color fundus photography (CFPh) were carried out with Topcon® OCT 2000 3D OCT as part of the standard care. Two patients were imaged on Topcon Atlantis® SS OCTA and one on Topcon Triton® SS OCTA. SS OCTA images were acquired using the 3 × 3 mm fovea-centered cubes scanning protocol. Analysis of both perifoveal superficial vascular plexus (pSVP) and perifoveal deep vascular plexus (pDVP) was performed by two observers after automated segmentation.

**Results:** Four eyes of three males (mean age 14 ± 3.8 years) were analyzed. All eyes showed foveoschisis on CFPh images. OCT B-scans of three eyes showed schistic cysts in the ganglion cell layer, inner nuclear layer (INL) and outer nuclear layer (ONL); in one eye, cysts were depicted in INL and ONL only. In two eyes, SS OCTA showed abnormal foveal avascular zone (FAZ) shape in the pSVP, and in the other two, FAZ shape was abnormal in both plexuses. In all eyes, retinal vascular abnormalities (ie, microvascular protrusions) were present in pDVP.

**Conclusion:** SS OCTA can depict perifoveal microvascular changes in young patients affected by XLRS. In this study, the structural and vascular changes seem to be more evident in the pDVP and may represent a useful biomarker of prognosis.

**Keywords:** retina, pediatric ophthalmology, swept source OCT, OCT angiography, X-linked retinoschisis

## Introduction

X-linked juvenile retinoschisis (XLRS; MIM 312700) is an inherited vitreoretinal degenerative disease, affecting almost exclusively males early in life.<sup>1</sup>

A total of 196 different mutations in the retinoschisin gene (RS1) have been identified to be responsible for XLRS.<sup>2</sup> The RS1 gene encodes a homo-oligomeric complex which binds the surface of photoreceptors and bipolar cells and helps them maintain the structural organization of the synapse. It may also play an important role in the regulation of the fluid balance between the intra- and extracellular space.<sup>3</sup>

Foveal schisis (intraretinal splitting) is present in 98–100% of patients, and it is ophthalmoscopically seen as a spoke-wheel pattern in the macular region. Vitreous and intraretinal hemorrhages have a prevalence of 30%, while retinal detachment occurs in up to 20% of patients.<sup>4</sup> In young patients affected by XLRS with exudative retinal

Correspondence: Francesco Stringa  
Central Manchester University Hospitals  
NHS Foundation Trust, Oxford Road,  
Manchester M13 9WL, UK  
Tel +44 161 701 7691  
Email francesco.stringa@cmft.nhs.uk

detachment or vitreous hemorrhage, several retinal vascular abnormalities have been found. These include perivascular sheathing, Coats-like exudative retinopathy and dendritiform vessels in the retinal periphery.<sup>5,6</sup>

Histopathological reports showed that the foveoschisis mainly occurs at the retinal nerve fiber layer (NFL) and ganglion cell layer (GCL).<sup>7,8</sup> However, studies using time-domain optical coherence tomography (OCT) systems have shown that foveomacular splitting can occur in different retinal layers, more often in the deeper retinal layers, rather than exclusively in the NFL and GCL.<sup>9–12</sup> These results have been corroborated by further evidence obtained with spectral domain (SD) OCT showing predominant localization of cysts at the inner nuclear layer (INL).<sup>13–15</sup>

The foveal avascular zone (FAZ) is a vessel-free region of the retina that is encircled by a fine capillary network. This region is responsible for central vision and fine visual acuity. Lesions within this site can cause severe vision loss.<sup>16</sup> Fundus fluorescein angiography (FFA) has shown FAZ enlargement and vascular leakage in patients with XLRS.<sup>17</sup> Nevertheless, FFA is an invasive technique, and dye injection can occasionally cause nausea or, more rarely, anaphylactic reactions.<sup>18</sup> General anesthesia may also be required for pediatric patients undergoing FFA, but there are insufficient data available to exclude the potentially negative influence of anesthesia on neurodevelopment in children.<sup>19</sup> Also, FFA provides bidimensional images where the fluorescent signal from retinal vascular networks can overlap or be obscured by leakage of fluorescein dye, therefore reducing the amount of information available to the clinician.

Recently, OCT angiography (OCTA) has been introduced into clinical practice. OCTA is a novel, noninvasive, static technique, which is able to detect blood flow by acquiring the de-correlation signal between consecutive OCT cross-sectional scans, repeated at the same location.<sup>20</sup> Additionally, OCTA can visualize retinal vascular plexuses, through a layer-by-layer analysis.<sup>21</sup>

Swept source OCTA (SS OCTA) provides a high 100-kHz A-line rate and deep signal penetration through the retina and choroid.<sup>22</sup> An innovative SS OCTA algorithm has been developed that improves the detection of reduced blood flow and motion artifacts without compromising axial resolution.<sup>23</sup>

The purpose of our study is to describe perifoveal microvascular abnormalities by using segmented SS OCTA imaging in young patients affected by XLRS in an attempt to provide novel information on this disease.

## Patients and methods

This is a retrospective observational case series. All information was routinely collected as part of standard care at

the Pediatric-Vitreoretinal Clinic, Manchester Royal Eye Hospital, Central Manchester University Hospitals NHS Foundation Trust, between October 2015 and April 2016. This study conformed to the tenets of the Declaration of Helsinki, and data were anonymized.

Three patients with XLRS were identified. The following data were collected to confirm XLRS diagnosis: patients' family history, personal medical history, genetic results and details of clinical examination. All eyes were imaged on Topcon® OCT 2000 3D OCT (Topcon Corporation, Tokyo, Japan) which provided structural OCT and color fundus photography (CFPh) images. Two patients were imaged on deep ranging imaging (DRI) OCT-1 Atlantis® SS OCTA, which is a 100-kHz SS OCTA system with a light spectrum source peaking at 1050 nm wavelength, and a digital resolution of 2 μm. One patient was imaged on DRI OCT Triton Plus® SS OCTA (Topcon Corporation) which has a central wavelength of 1050 nm, an acquisition speed of 100,000 A-scans per second and an axial and transversal resolution of 7 and 20 μm in tissue, respectively. Triton Plus was not available at the beginning of this study. One of its advantages compared to previous devices is that it has SMART Track® eye tracking system that provides better image quality and less background noise.<sup>23</sup>

All OCTA images were acquired from 3 × 3 mm scanning cubes with each cube consisting of 320 clusters of B-scans centered on the fovea. Central retinal thickness (CRT) was automatically calculated using the Topcon® OCT 2000 3D OCT mapping software. OCT angiograms were generated with the following automated segmentation: the perifoveal superficial vascular plexus (pSVP), from the internal limiting membrane to the boundary between the inner plexiform layer (IPL) and the inner nuclear layer (INL); the perifoveal deep vascular plexus (pDVP), from the boundary between IPL and INL to the boundary between the outer plexiform layer and the outer nuclear layer (ONL). Imaging analysis was performed with IMAGENet® (version 1.19) when images were acquired with Triton Plus and with Atlantis SS OCTA custom built software when images were acquired with Atlantis.

All images were independently reviewed by two ophthalmologists (PES and AJ). Observers were questioned about the absence or presence and location of intraretinal cysts on OCT B-scans. Intraretinal cysts were defined as the occurrence of round or oval hyporeflective spaces at the level of GCL, INL or ONL on structural OCT images. The examiners were, also, questioned about the absence or presence and location (whether in pSVP or pDVP) of microvascular changes (ie, microvascular protrusions). These were defined

as the presence of expanded and tortuous hyperreflective capillaries within the pSVP and/or pDVP on en face OCTA images. Finally, the FAZ shape was judged to be abnormal if interruption of perifoveal capillaries was evident on en face OCT angiograms.

## Ethical approval

This study was approved by the Central Manchester Local Research Ethics Committee. The patients' consent to review their medical records was not required by the institutional review board.

## Results

Four eyes from three patients (mean age  $14 \pm 3.8$  years) with previous diagnosis of XLRS were included. All reviewers were in agreement in regard to intraretinal cyst location, microvascular changes and FAZ shape abnormalities.

### Patient 1

This patient showed to have the RS1 gene mutation c.487 T>C (p.W163R) (Exon 5). In both eyes, funduscopy examination showed stellate spoke-like maculopathy. Best-corrected visual acuity (BCVA) was, respectively, 6/12 in the right eye and 6/9 in the left. No submacular hemorrhage, exudation or preretinal/subretinal fibrosis was evident in either eye. Structural OCT B-scans showed foveal schistic cysts

localized in the GCL, INL (bigger at this level) and ONL. CRT was 262  $\mu\text{m}$  in the right eye and 260  $\mu\text{m}$  in the left. SS OCTA images were acquired with Atlantis. No microvascular changes were seen in the pSVPs in both eyes. However, abnormal microvascular protrusions were identified in both pDVPs. In the right eye, the FAZ shape was judged normal in pSVP and abnormal in pDVP. In the left eye, FAZ shape was abnormal in both plexuses (Figure 1).

### Patient 2

This patient presented with the RS1 gene mutation c.590 G>A (p.R197H) (Exon 6). Imaging analysis of the data acquired from the left eye was unsuccessful because of retinal detachment involving the fovea. In the right eye, BCVA was 6/12, and funduscopy examination showed stellate spoke-like maculopathy with perimacular exudation. Inferior peripheral retinoschisis with bridging vessels between retinal leaflets was also present. Structural OCT B-scans showed high retinal disruption and foveal schistic cysts localized in the GCL, INL (bigger in the INL) and ONL. Right eye's CRT was 340  $\mu\text{m}$ . OCTA images were acquired with Atlantis. There were no microvascular changes in the pSVP. Vessels with abnormal protrusion and course were identified in pDVP. A single vascular abnormality has been observed at the boundary between the pSVP and pDVP. The FAZ shape was abnormal in both plexuses (Figure 2).

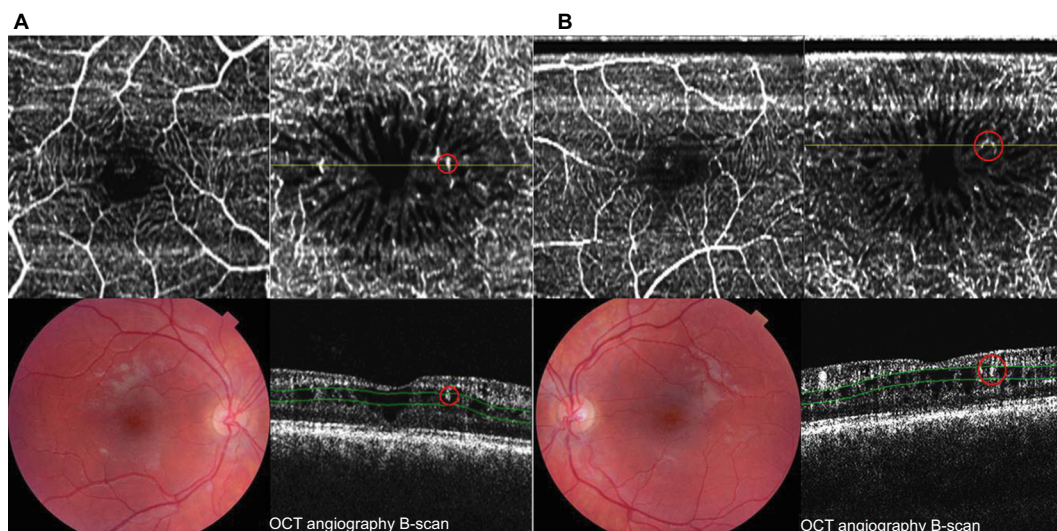


**Figure 1** Observations in patient 1. **(A)** Right eye (left side):  $3 \times 3$  mm fovea-centered OCTA image of pSVP (upper left) shows no perifoveal capillary network interruptions. Hyperreflective retinal abnormalities (ie, microvascular protrusions in red circle) within enlarged foveal avascular zone in the pDVP (upper right). B-scan image (lower right) shows perifoveal-nasal dilated capillary within a schisis cavity (red circle). **(B)** Left eye (right side):  $3 \times 3$  mm fovea-centered OCTA image of pSVP (upper left) shows inferior-perifoveal capillary network interruption. Hyperreflective retinal abnormalities (ie, microvascular protrusions in red circle) within enlarged foveal avascular zone in the pDVP (upper right). B-scan image (lower right) shows perifoveal-temporal dilated capillaries within a schisis cavity (red circle). Copyright © 2016 Karger Publishers, Basel, Switzerland. Adapted with permission from Stanga PE, Papayannis A, Tsamis E, et al. Swept-source optical coherence tomography angiography of paediatric macular diseases. *Dev Ophthalmol*. 2016;56:166–173.<sup>25</sup>

**Abbreviations:** OCTA, optical coherence tomography angiography; pSVP, perifoveal superficial vascular plexus; pDVP, perifoveal deep vascular plexus.

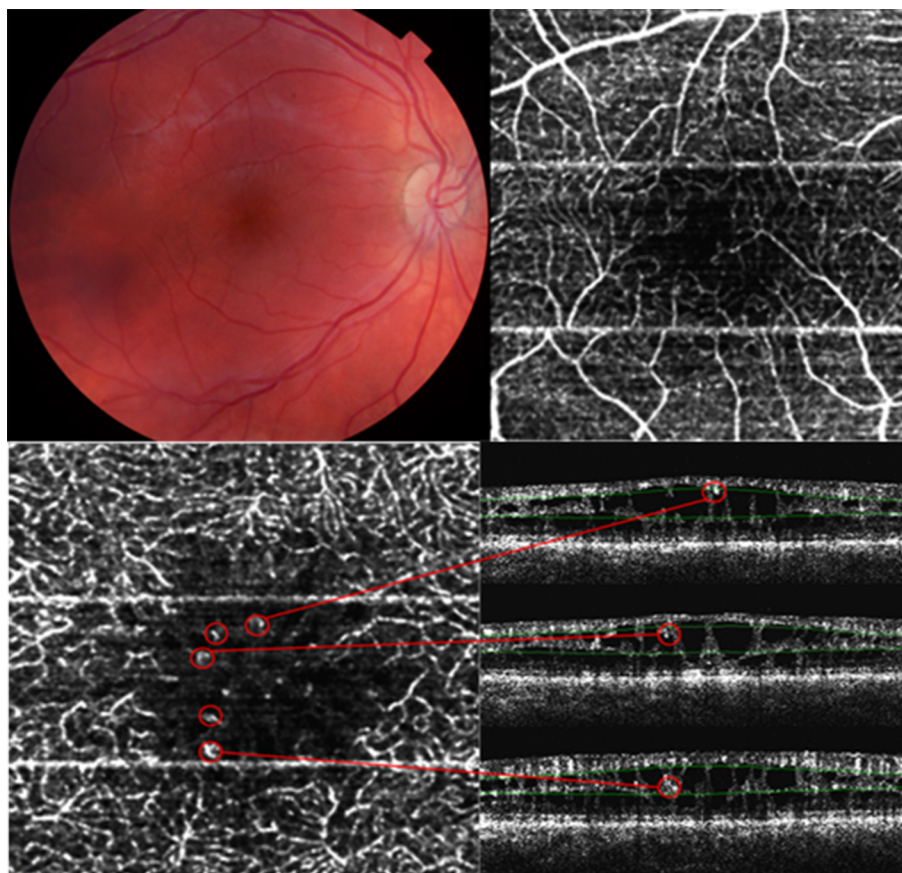


**Figure 2** Observations in patient 2. Right eye: Perifoveal superficial vascular plexus in a  $3 \times 3$  mm fovea-centered OCTA image with inferior interruption of the capillary network (upper right). Hyperreflective retinal abnormalities (ie, microvascular protrusions; red circles) within enlarged foveal avascular zone in the pDVP en face OCTA and B-scan images (lower band of images). Note the vascular retinal abnormality at the boundary between pSVP and pDVP on the upper B-scan image (red circle). Copyright © 2016 Karger Publishers, Basel, Switzerland. Adapted with permission from Stanga PE, Papayannis A, Tsamis E, et al. Swept-source optical coherence tomography angiography of paediatric macular diseases. *Dev Ophthalmol*. 2016;56:166–173.<sup>25</sup>

**Abbreviations:** OCTA, optical coherence tomography angiography; pDVP, perifoveal deep vascular plexus; pSVP, perifoveal superficial vascular plexus.

### Patient 3

This patient presented with the RS1 gene mutation c.214 G>A (p.E72K) (Exon 4). Imaging analysis of the left eye was not possible because of vitreous hemorrhage. Clinical examination of the right eye showed a BCVA of 6/9 and stellate spoke-like maculopathy with no retinal exudation. Structural OCT B-scans showed intraretinal cysts localized in both INL and ONL, with CRT of 295  $\mu\text{m}$ . SS OCTA images were acquired with Triton Plus. Microvascular changes were evident in the pDVP only. The FAZ shape was abnormal in both plexuses (Figure 3).

### Discussion

Despite the well-established clinical appearance of XLRS, the precise mechanism of the schisis cysts formation is still a topic of debate. Identification of RS1 gene and its cell–cell adhesive properties between bipolar and photoreceptor cells suggested that the schisis could be generated by loss of adhesion between retinal layers.<sup>3</sup> Joshi et al speculated that the intraretinal cavities formation could be the result of

intrastructural retinal defects combined with vitreous tractional forces.<sup>24</sup> Also, Molday et al pointed out that interactions between mutated RS1 and Na/K<sup>+</sup> ATPase pumps may alter the ionic gradient and tissue balance resulting in extracellular fluid accumulation in intraretinal cysts.<sup>2</sup>

Previous case reports have shown retinal vascular changes such as Coats-like exudative retinopathy, perivascular sheathing and peripheral dendritiform vascular alterations in patients with XLRS complicated by exudative retinal detachment, and vitreous and intraretinal hemorrhage.<sup>6</sup> It has been hypothesized that retinal vessels between the schistic cysts may be more sensitive to mechanical stress because of lack of the glial support. This could lead to alteration of blood–retinal barrier and, consequently, to vitreous hemorrhage and exudative retinal detachment, which are the most frequent sight-threatening complications in XLRS.<sup>7</sup>

In this article, we described retinal structural abnormalities and perifoveal microvascular changes with SS OCTA in patients with XLRS. In all eyes, the schisis cavities are more evident in the ONL and INL, mainly in the latter, and this was

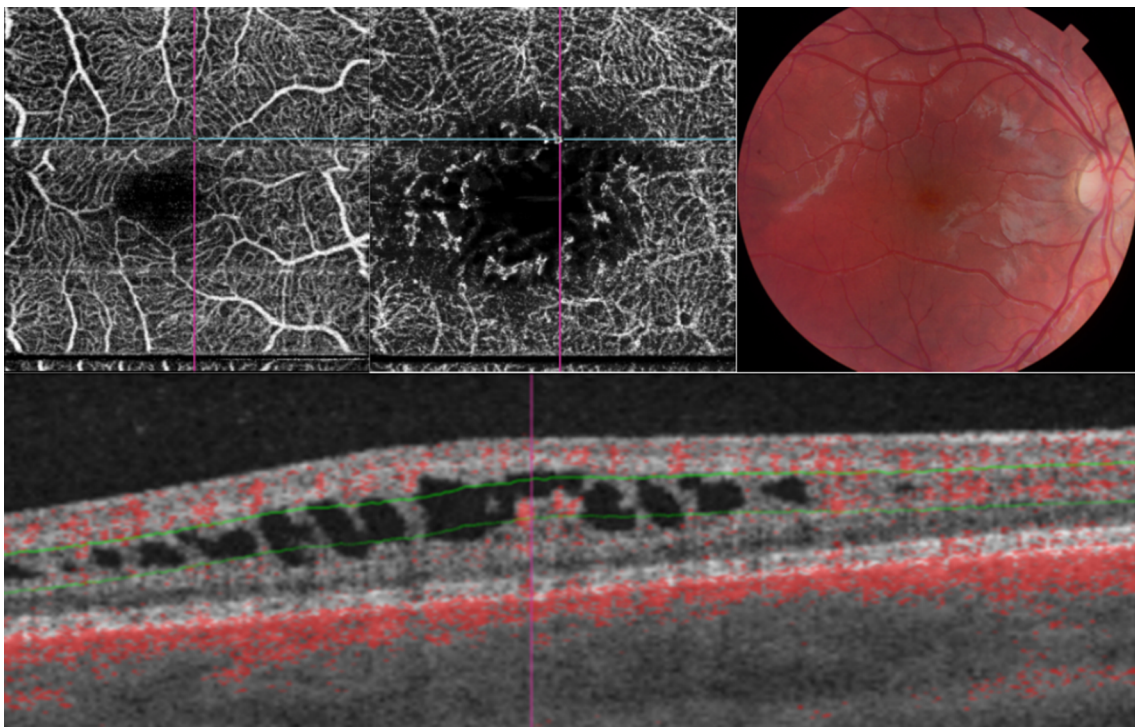


**Figure 3** Observations in patient 3. Perifoveal superficial vascular plexus in a  $3 \times 3$  mm fovea-centered OCTA image with supero-nasal interruption of the capillary network (upper left). Hyperreflective retinal abnormalities (ie, microvascular protrusions) within enlarged foveal avascular zone in the pDVP (upper central). B-scan image centered on a dilated capillary shows lack of glial support and protrusion in a schisis cavity in the pDVP. Vascular flow is automatically represented with red color by IMAGEnet®.

**Abbreviations:** OCTA, optical coherence tomography angiography; pDVP, perifoveal deep vascular plexus.

also reported in previous studies.<sup>13–15</sup> We believe that retinal cavities location could be related with the RS1's propriety to lead structural adhesion between bipolar cells and photoreceptors, that is, in between INL (anteriorly) and ONL (posteriorly).

Interruption of the superficial perifoveal microvasculature was evident on SS OCTA images in two out of four eyes, whereas in the pDVP, the interruption was observed in all eyes. FAZ enlargement has also been recently described with FFA by Rao et al in seven out of 36 eyes of patients with XLRS.<sup>17</sup> However, we believe that the number of eyes with FAZ enlargement in the pDVP might have been higher, because FFA is a single-plane imaging modality and a clear visualization of the small retinal vessels beneath the superficial plexus is not always possible.

Our study group has previously described microvascular abnormalities resembling telangiectasia in both perifoveal plexuses of young patients with X-linked retinoschisis.<sup>25</sup> However, the above-mentioned findings were observed with an SD device that did not benefit from being paired with SS technology and misinterpretation of the results might have occurred. In this present study, patients 1 and 2, who had been imaged with DRI Atlantis SD OCTA, were imaged with an updated version of DRI Atlantis SS OCTA which provided a better imaging resolution and a more accurate analysis. In all

eyes, microvascular abnormalities on pDVP OCTA images were observed. We have described these changes as abnormal protrusions of the microvascular walls and tortuosity of the vessels' course. However, none of them were evident on ophthalmic examination, nor on CFPh. SS OCTA B-scan images showed that these vascular abnormalities were located in pillar-like structures between schisis cavities, with a limited glial support and surrounded by intraretinal fluid (Figure 3). Interestingly, no microvascular protrusions were observed in the pSVP. In patient 2, a microvascular protrusion seemed to be placed in between the pSVP and pDVP. We believe that the capillaries located at the inner and external border of the INL, which have a smaller diameter,<sup>26</sup> could be more sensitive to tractional stress compared to those located in the NFL. However, whether these vascular changes were due to a primary weakness of the microvascular walls or secondary to mechanical forces caused by intraretinal fluid accumulation is hard to say. A combination of the two mechanisms might be possible.

There are some limitations in our study that should be considered. First of all, the sample size is limited, and there is no control group. Secondly, we adopted a  $3 \times 3$  mm fovea-centered scanning modality, which was limited to the perifoveal area. Wider scanning areas could provide more information on the peripheral retinal vasculature.

Additionally, the background noise of current OCTA devices could have influenced the imaging analysis (eg, segmentation, vascular flow analysis).

The above-described perifoveal retinal features (schisis cavities, perifoveal vascular network interruptions and microvascular protrusions) seemed to be located more often in the pDVP. Therefore, imaging techniques that provide layer-by-layer analysis, such as OCTA, could have an advantage over single-plane imaging modalities, such as FFA. In this study, data were obtained with SS OCTA, which has a light source centered at 1050 nm and can penetrate tissues to a greater extent with less sensitivity roll-off with depth compared to SD OCT. This represents a potential advantage when imaging eyes with media opacities and edematous retinas such as in XLRS. Finally, images acquired with Triton Plus SS OCTA, that benefits from being updated with SMART Track eye tracking system and therefore providing a higher image resolution, confirmed perifoveal changes observed with the Atlantis SS OCTA in patients 1 and 2.

## Conclusion

SS OCTA is a noninvasive imaging technique that can provide clinically useful information on the perifoveal vasculature even in conditions of retinal disorganization, such as foveal schisis. The described microvascular changes may play a role in the pathogenesis of schisis cyst formation, intraretinal hemorrhage and retinal detachment. Therefore, SS OCTA could be used as part of the standard care for the diagnosis and the follow-up of patients affected by XLRS.

## Author contributions

All authors contributed towards data analysis, drafting and critically revising the paper and agree to be accountable for all aspects of the work.

## Disclosure

Paulo Eduardo Stanga is a consultant of Topcon Corporation, Tokyo, Japan. The other authors report no conflicts of interest in this work.

## References

- Ide CH, Wilson RJ. Juvenile retinoschisis. *Br J Ophthalmol*. 1973;57(8):560–562.
- Molday RS, Kellner U, Weber BHF. X-linked juvenile retinoschisis: clinical diagnosis, genetic analysis, and molecular mechanisms. *Prog Retin Eye Res*. 2012;31(3):195–212.
- Wu WW, Wong JP, Kast J, Molday RS. RS1, a discoidin domain-containing retinal cell adhesion protein associated with X-linked retinoschisis, exists as a novel disulfide-linked octamer. *J Biol Chem*. 2005;280(11):10721–10730.
- Sikkink SK, Biswas S, Parry NR, Stanga PE, Trump D. X-linked retinoschisis: an update. *J Med Genet*. 2007;44(4):225–232.
- Fong DS, Frederick AR Jr, Blumenkranz MS, Walton DS. Exudative retinal detachment in X-linked retinoschisis. *Ophthalmic Surg Lasers*. 1998;29(4):332–335.
- Greven CM, Moreno RJ, Tasman W. Unusual manifestations of X-linked retinoschisis. *Trans Am Ophthalmol Soc*. 1990;88:211–225.
- Yanoff M, Kertesz Rahn E, Zimmerman LE. Histopathology of juvenile retinoschisis. *Arch Ophthalmol*. 1968;79(1):49–53.
- Condon GP, Brownstein S, Wang NS, Kearns JA, Ewing CC. Congenital hereditary (juvenile X-linked) retinoschisis. Histopathologic and ultrastructural findings in three eyes. *Arch Ophthalmol*. 1986;104(4):576–583.
- Azzolini C, Pierro L, Codenotti M, Brancato R. OCT images and surgery of juvenile macular retinoschisis. *Eur J Ophthalmol*. 1997;7(2):196–200.
- Yu J, Ni Y, Keane PA, Jiang C, Wang W, Xu G. Foveomacular schisis in juvenile X-linked retinoschisis: an optical coherence tomography study. *Am J Ophthalmol*. 2010;149(6):973–978.
- Brucker AJ, Spaide RF, Gross N, Klancnik J, Noble K. Optical coherence tomography of X-linked retinoschisis. *Retina*. 2004;24(1):151–152.
- Azzolini C, Sansoni G, Donati S, et al. Clinical analysis of macular edema with new software for SD-OCT imaging. *Eur J Ophthalmol*. 2013;23(6):899–904.
- Apushkin MA, Fishman GA, Janowicz MJ. Correlation of optical coherence tomography findings with visual acuity and macular lesions in patients with X-linked retinoschisis. *Ophthalmology*. 2005;112(3):495–501.
- Gregori NZ, Berrocal AM, Gregori G, et al. Macular spectral-domain optical coherence tomography in patients with X linked retinoschisis. *Br J Ophthalmol*. 2009;93(3):373–378.
- Biswas S, Funnell CL, Gray J, Bunting R, Lloyd IC, Stanga PE. Nidek MP-1 microperimetry and Fourier domain optical coherence tomography (FD-OCT) in X linked retinoschisis. *Br J Ophthalmol*. 2010;94(7):949–950.
- Song H, Zhao Y, Qi X, Chui YT, Burns SA. Stokes vector analysis of adaptive optics images of the retina. *Opt Lett*. 2008;33(2):137–139.
- Rao P, Robinson J, Yonekawa Y, et al. Wide-field imaging of nonexudative and exudative congenital X-linked retinoschisis. *Retina*. 2016;36(6):1093–1100.
- Kwiterovich KA, Maguire MG, Murphy RP, et al. Frequency of adverse systemic reactions after fluorescein angiography. Results of a prospective study. *Ophthalmology*. 1991;98(7):1139–1142.
- Lee JH, Zang J, Wei L, Yu SP. Neurodevelopmental implications of the general anesthesia in neonate and infants. *Exp Neurol*. 2015;272:50–60.
- Jia Y, Bailey ST, Wilson DJ, et al. Quantitative optical coherence tomography angiography of choroidal neovascularization in age-related macular degeneration. *Ophthalmology*. 2014;121(7):1435–1444.
- Spaide RF, Klancnik JM Jr, Cooney MJ. Retinal vascular layers imaged by fluorescein angiography and optical coherence tomography angiography. *JAMA Ophthalmol*. 2015;133(1):45–50.
- Huang Y, Zhang Q, Thorell MR, et al. Swept-source OCT angiography of the retinal vasculature using intensity differentiation-based OMAG algorithms. *Ophthalmic Surg Lasers Imaging Retina*. 2014;45(5):382–389.
- Stanga PE, Tsamis E, Papayannis A, Stringa F, Cole T, Jalil A. Swept-Source Optical Coherence Tomography Angio™ (Topcon Corp, Japan): technology review. *Dev Ophthalmol*. 2016;56:13–17.
- Joshi MM, Drenser K, Hartzler M, Dailey W, Capone A Jr, Trese MT. Intrachisis cavity fluid composition in congenital X-linked retinoschisis. *Retina*. 2006;26 (Suppl 7):S57–S60.
- Stanga PE, Papayannis A, Tsamis E, et al. Swept-source optical coherence tomography angiography of paediatric macular diseases. *Dev Ophthalmol*. 2016;56:166–173.
- Snodderly DM, Weinhaus RS. Retinal vasculature of the fovea of the squirrel monkey, *Saimiri sciureus*: three-dimensional architecture, visual screening and relationships to the neuronal layers. *J Comp Neurol*. 1990;297:145–163.

### International Medical Case Reports Journal

Dovepress

#### Publish your work in this journal

The International Medical Case Reports Journal is an international, peer-reviewed open-access journal publishing original case reports from all medical specialties. Previously unpublished medical posters are also accepted relating to any area of clinical or preclinical science. Submissions should not normally exceed 2,000 words or

4 published pages including figures, diagrams and references. The manuscript management system is completely online and includes a very quick and fair peer-review system, which is all easy to use. Visit <http://www.dovepress.com/testimonials.php> to read real quotes from published authors.

Submit your manuscript here: <https://www.dovepress.com/international-medical-case-reports-journal-journal>